Science Advances
AAAS

advances.sciencemag.org/cgi/content/full/5/12/eaay2670/DC1

Supplementary Materials for

The long noncoding RNA *neuroLNC* regulates presynaptic activity by interacting with the neurodegeneration-associated protein TDP-43

S. Keihani, V. Kluever, S. Mandad, V. Bansal, R. Rahman, E. Fritsch, L. Caldi Gomes, A. Gärtner, S. Kügler, H. Urlaub, J. D. Wren, S. Bonn, S. O. Rizzoli, E. F. Fornasiero*

*Corresponding author. Email: efornas@gwdg.de

Published 18 December 2019, *Sci. Adv.* **5**, eaay2670 (2019)
DOI: 10.1126/sciadv.aay2670

The PDF file includes:

Other Supplementary Material for this manuscript includes the following:

(available at advances.sciencemag.org/cgi/content/full/5/12/eaay2670/DC1)

Data S1 (Microsoft Excel format). Summary of data used here, see first sheet for details.

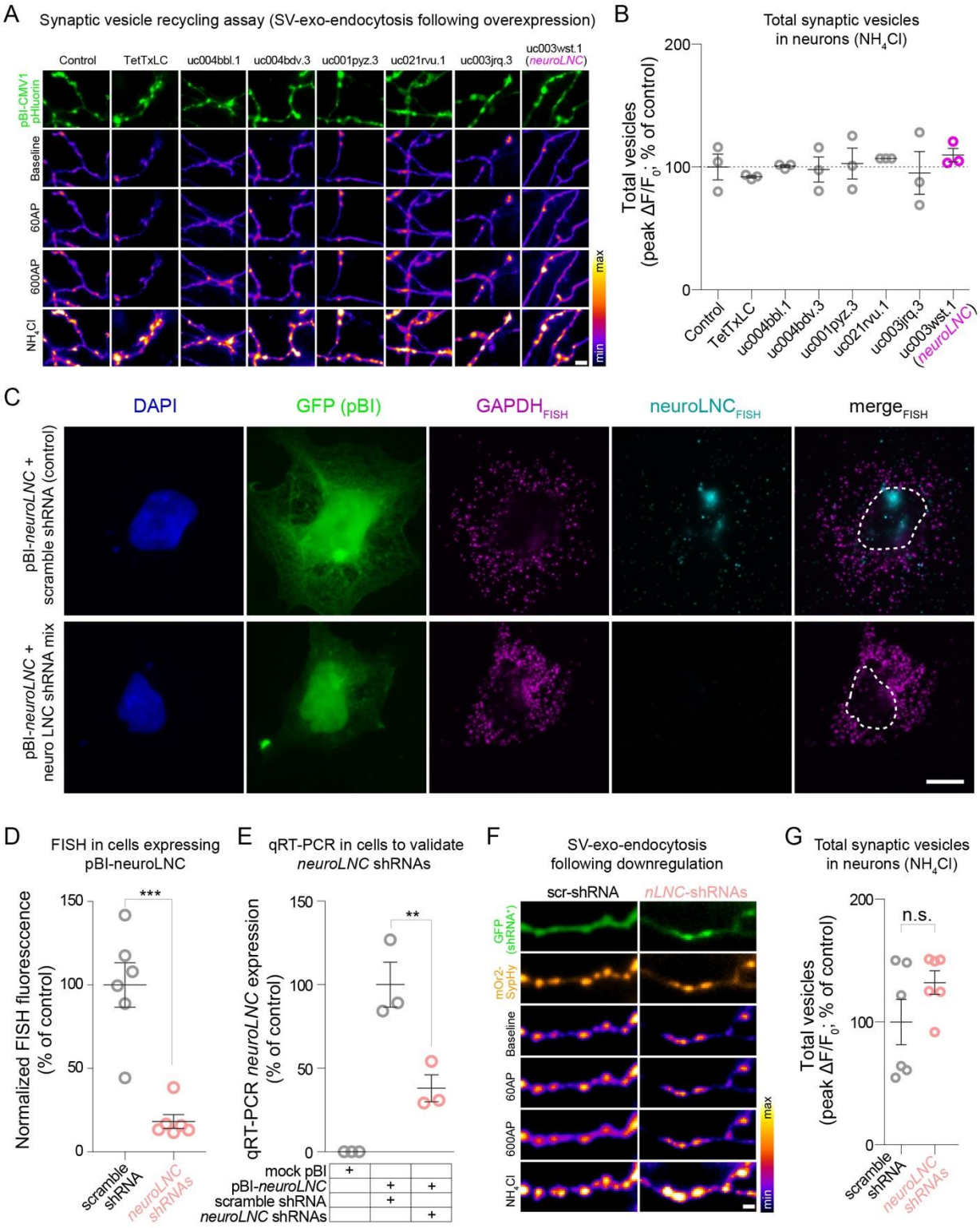

Fig. S1. Details of the screening strategy used for studying the role of lncRNAs in neuronal activity and down-regulation in culture. (**A**) Exemplary images of the synaptic vesicle recycling assay used for screening the 6 most promising lncRNAs. Neurons were transfected with the bidirectional pBI-pHluorin plasmids to modulate synaptic activity at >14 DIV. Optical

methods for measuring exocytosis and endocytosis of synaptic vesicles are very useful and relatively simple to implement (*15*). The pHluorin based on VAMP2 uses a pH-dependent GFP which is normally quenched at low pH inside synaptic vesicles (pH ~ 5.4). Following stimulation, vesicles fuse with the plasma membrane and the internal pH of the vesicle equilibrates with Tyrode's solution pH (7.4). 60 and 600 action potentials at 20 Hz have been used for testing the neuronal response, observed by fluorescence increase in the GFP channel. At the end of each experiment, with ammonium chloride (NH_4Cl) it is possible to unquench all the GFP molecules that were not used during recycling, thus revealing the total pool of vesicles. Neuron expressing uc003wst.1 (*neuroLNC*) show a clear increase in synaptic exo-endocytosis at both stimulations. Scale bar 2 μm. (**B**) Quantification of the total amount of synaptic vesicles for the experiments quantified in main **Figs. 1B** and **1C**. Mean values normalized by the initial fluorescence (F_0) are plotted (± s.e.m.). Statistical test: one-way ANOVA followed by Bonferroni's multiple comparison test *vs*. control (no significant differences were found). (**C**) Control of efficiency of *neuroLNC* downregulation in HEK293 cells transfected with pBI-*neuroLNC* and either a scramble control RNA or a mix of shRNAs against *neuroLNC* as detailed in Methods and **Data S1J**. The exemplary images show the GFP fluorescence and the RNA fluorescence in situ hybridization (RNA-FISH) for both GAPDH (as a control) and *neuroLNC*. Note that the shRNA mix downregulation ablates *neuroLNC* expression. Scale bar 10 μm. (**D**) Fluorescence quantification of the experiment summarized in **C**. Downregulated cells that are positive for pBI-*neuroLNC* show a highly significant downregulation of *neuroLNC* expression. Statistical test: two-tailed Student t-test (*** $P < 0.001$). (**E**) qRT-PCR of the samples transfected as indicated in the scheme in the lower portion of the graph. Mean values of *neuroLNC* normalized to GAPDH and expressed as a percentage of the control expressing the pBI-*neuroLNC* and the scramble shRNA are plotted (± s.e.m.). The downregulation is confirmed also by qRT-PCR. Note that in this case the downregulation of *neuroLNC* might be in part attenuated by cells which expressed the pBI-*neuroLNC* but not the shRNA mix. Statistical test: one-way ANOVA followed by Bonferroni's multiple comparison test vs. reference (** $P < 0.01$). (**F**) Exemplary images of the synaptic vesicle recycling in *neuroLNC* downregulated neurons, similar to panel **A**. In this case neurons co-transfected with the shRNAs and the orange version of the pH-dependent synaptic vesicle sensor mOr2-SypHy (*21*) were imaged. (**G**) Quantification of the total amount of synaptic vesicles for the experiments quantified in main **Fig. 1D** and **1E**, quantified and analyzed as in panel **B**. The downregulation does not influence the total number of synaptic vesicles.

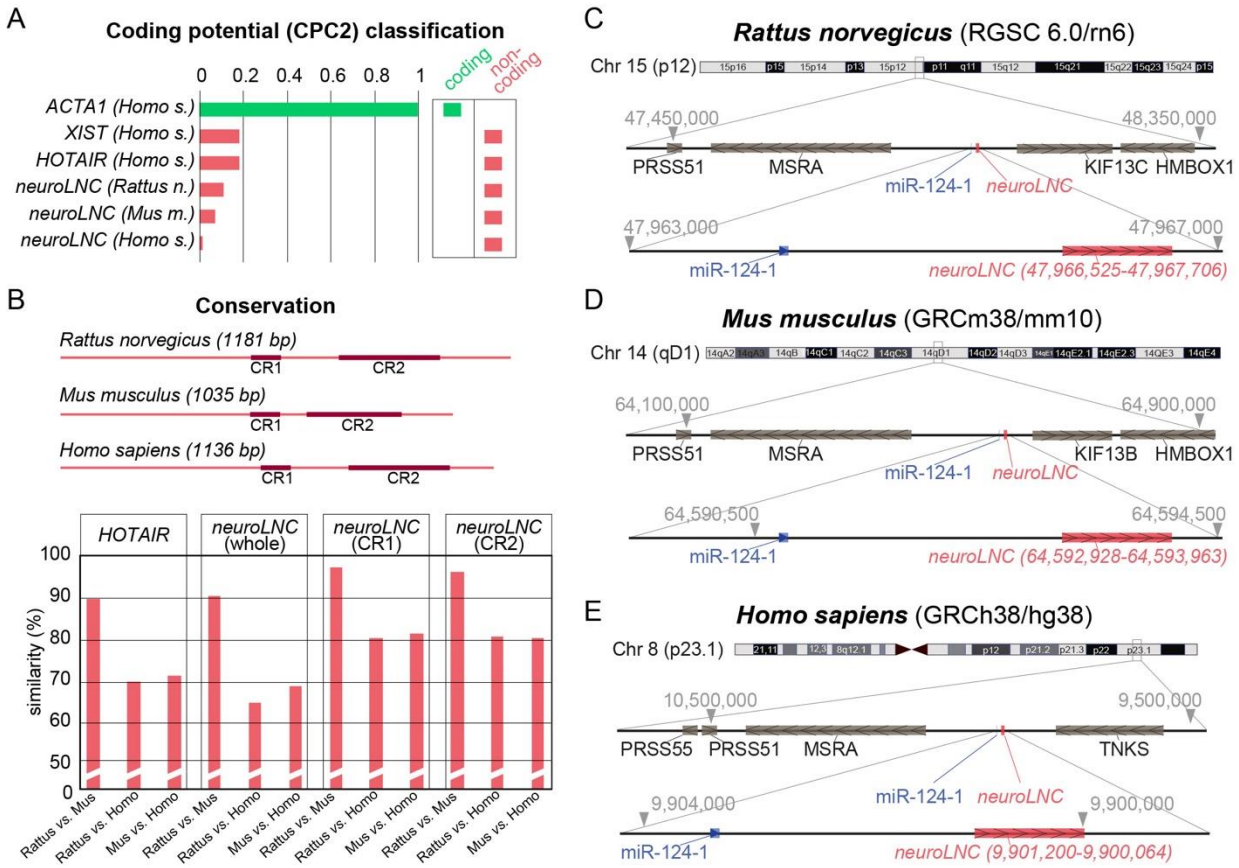

Fig. S2. *NeuroLNC* coding potential, conservation, and locus organization. (**A**) Coding potential evaluation of *neuroLNC* in rat, mouse and human as previously described (*39*). The coding potential of the mRNA for alpha 1 actin and of two famous lncRNAs (XIST and HOTAIR) are used as a reference. The coding potential of *neuroLNC* in rat, mouse and human is extremely low and in the three organisms the lncRNAs can be considered *bona fide* non-coding constructs. (**B**) Conservation analysis of *neuroLNC* in rat, mouse and human as defined in **Data S1B**. The positioning of the two conserved regions (CR1 and CR2) are represented in the scheme (upper part of the panel). Similarity is detailed for the three possible pairs across the three different organisms (rat *vs.* mouse, mouse *vs.* human and rat *vs.* human). The percentage of similarity across orthologous lncRNAs is lower than the similarity observed for coding sequences. We also report the similarities for HOTAIR. *NeuroLNC* shows a relatively high conservation across these organisms, especially within *CR1* and *CR2* regions, which have similarities >80% even between rodents and humans. (**C-E**) Schematic representation of the genomic locus of *neuroLNC* for rat, mouse and human with additional details in respect to **Fig. 1F**. Chromosomal localizations are specified with gray arrowheads and numbers. For details about reference genomic assemblies and localizations please refer to **Data S1B**.

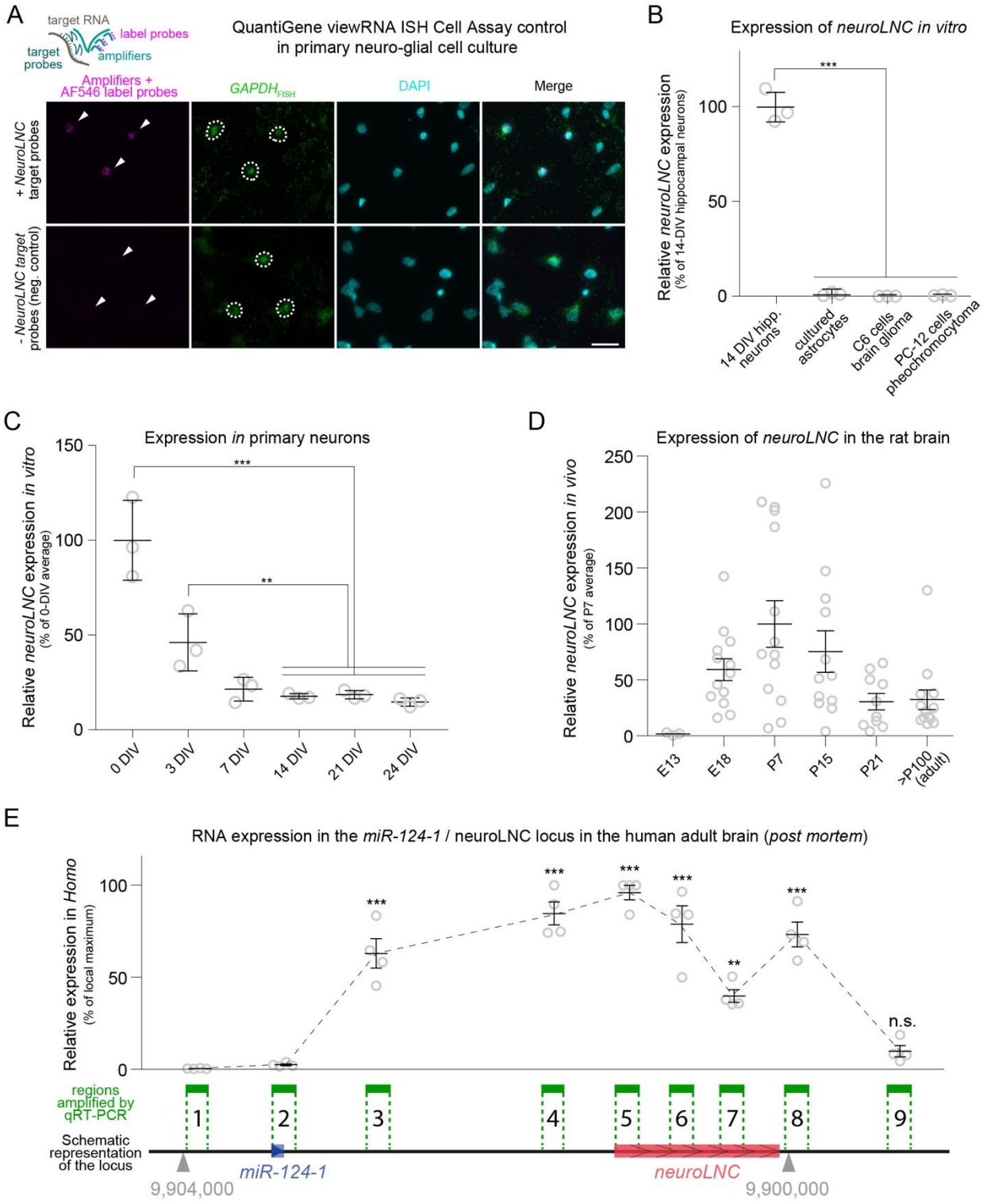

Fig. S3. Specificity of the RNA-FISH approach and expression of *neuroLNC* in rodent cultures and in adult human brain. (**A**) RNA-FISH on mixed neuroglia cultures against *neuroLNC* in the presence or in the absence of the specific target probes (respectively upper and lower panels). Upper left corner: schematic representation of the approach summarizes the functioning of the "QuantiGene ViewRNA" ISH Cell Assay kit (Affymetrix). Briefly, two target

probes ensure the coincidence detection which is necessary for achieving signal amplification through the set of amplifiers and label probes. The RNA-FISH for GAPDH is used as an internal control for the correct annealing of all targets. Note that in our cultures, neurons are easily spotted by the fact that GAPDH is concentrated in the cell soma (segmented white lines), while flat glial cells that function as a feeder-layer in these cultures have a much less concentrated GAPDH distribution. In the presence of target probes, the cell soma of neurons (segmented white lines) is positive for *neuroLNC*, while in the absence of target probes there is basically no detectable signal. Scale bar 30 μm. (**B**) Relative *neuroLNC* expression by qRT-PCR in hippocampal neurons at 14 days in vitro (DIV) neurons *vs.* primary cultures astrocytes, C6 or PC-12 cells. The expression of *neuroLNC* is virtually non-detectable in non-neuronal cells. Statistical test: one-way ANOVA followed by Bonferroni's multiple comparison test *vs.* non-neuronal samples (*** $P < 0.001$). (**C**) Developmental regulation of *neuroLNC* in primary hippocampal neurons. Right after plating at 0 DIV, the expression of *neuroLNC* is relatively higher than at other developmental stages in culture. Note that, although lower, the expression in terminally differentiated cells is in any case much higher than in other cell types (for comparison refer to panel **B**, where the 14 DIV sample is used as a control against non-neuronal cells). Statistical test: one-way ANOVA followed by Bonferroni's multiple comparison test *vs.* non-neuronal samples (** $P < 0.01$ and *** $P < 0.001$). (**D**) Developmental regulation of *neuroLNC* in rat brain assessed by qRT-PCR, normalized to GAPDH and expressed as a percentage of the expression peak at P7. The expression of *neuroLNC* is virtually absent at E13, when also most of the mRNAs linked with neuronal terminal differentiation are absent. The expression peaks at P7 and decreases later in development and in the adult. (**E**) Relative RNA amounts in the *miR-124-1 / neuroLNC* locus in post mortem human brain. The levels of RNAs detected with qRT-PCR are normalized to GAPDH and plotted as percentage of the maximum peak in the locus. The cDNA used for qRT-PCR originated from the midbrain. Statistical test: one-way ANOVA followed by Bonferroni's multiple comparison test *vs.* regions 1 and 2 (*** $P < 0.001$).

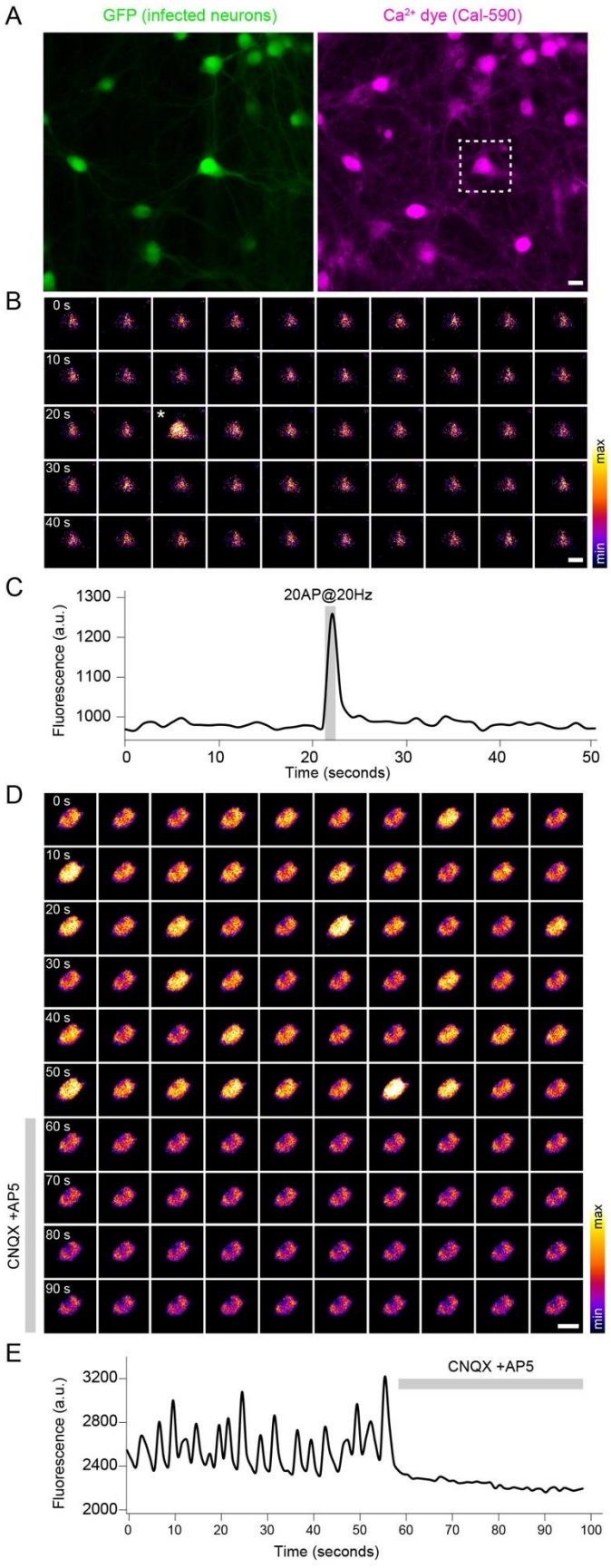
A
GFP (infected neurons)
Ca2+ dye (Cal-590)
B
0 s
10 s
20 s
30 s
40 s
max
min
C
20AP@20Hz
Fluorescence (a.u.)
1300
1200
1100
1000
0
10
20
30
40
50
Time (seconds)
D
0 s
10 s
20 s
30 s
40 s
50 s
60 s
70 s
80 s
90 s
CNQX +AP5
max
min
E
CNQX +AP5
Fluorescence (a.u.)
3200
2800
2400
2000
0
10
20
30
40
50
60
70
80
90
100
Time (seconds)

Fig. S4. Controls for the calcium dynamics experiments. (**A**) Infected neurons (upper green panel) were loaded with the Ca^{2+} dye Cal-590-AM (magenta), placed in a stimulation chamber and stimulated with different frequencies. Scale bar 10 µm. (**B**) Exemplary Ca^{2+} signal from the neuron in the segmented white line from panel **A**. During the time-lapse experiment the neuron was stimulated with 20AP at 20 Hz. Upon stimulation, (indicated in the image with an asterisk) the fluorescence of the Cal-590 dye increases and the calcium influx can be measured. Scale bar 10 µm. (**C**) Quantification of the fluorescence change from panel **B**. (**D**) Exemplary Ca^{2+} signal of a spontaneously active neuron loaded with Cal-590-AM. Scale bar 10 µm. Upon treatment with 10 µM CNQX (an AMPA/kainate receptor antagonist) and 50 µM D-AP5 (an NMDA receptor antagonist), the spontaneous activity is abolished, as shown by the block of calcium fluctuations, quantified in panel **E**. Scale bar 10 µm.

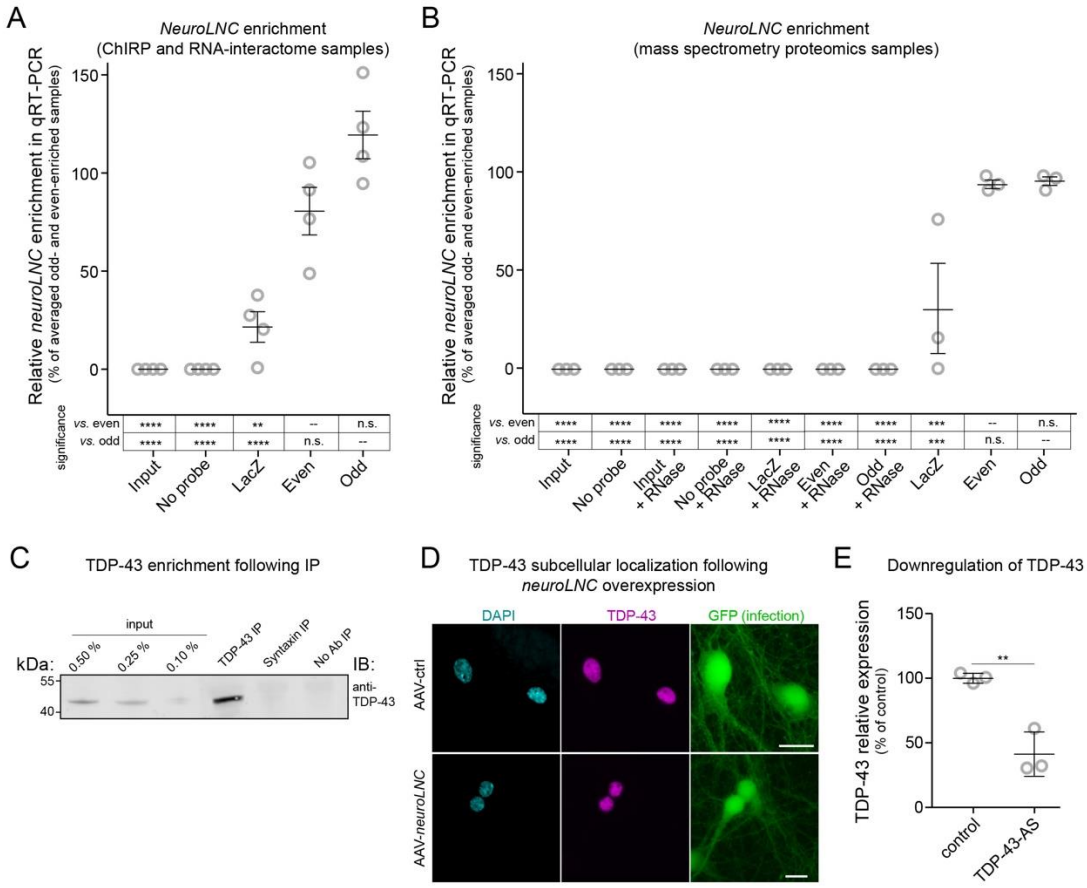

Fig. S5. Controls and additional information concerning Fig. 5. (**A**) *NeuroLNC* is specifically enriched in ChIRP and RNA-interactome in Even and Odd samples *vs.* all other samples. The qRT-PCR results for *neuroLNC* have been normalized to the respective GAPDH controls and are expressed as percentage of the averaged values of enriched samples. Statistical test: one-way ANOVA followed by Bonferroni's multiple comparison test as summarized in the significance table in the lower part of the graph (** $P < 0.01$ and **** $P < 0.0001$). (**B**) *NeuroLNC* enrichment as in **A**, for mass spectrometry proteomics samples. Statistical test: one-way ANOVA followed by Bonferroni's multiple comparison test as summarized in the significance table in the lower part of the graph (*** $P < 0.001$ and **** $P < 0.0001$). (**C**) Western blot confirming the enrichment of TDP-43 following its immunoprecipitation (IP). Immunoprecipitation with an anti-Syntaxin 1a antibody was used as a negative control. The membrane was immunoblotted (IB) with an anti-TDP-43 antibody, revealing a specific band at ~43 kDa in the lane were the TDP-43 IP was loaded. (**D**) Representative TDP-43 immunofluorescence of primary hippocampal neurons infected either with a control adeno-associated virus (AAV-ctrl) or a virus overexpressing *neuroLNC* (AAV-*neuroLNC*). Both viruses have a synapsin-GFP reporter cassette, allowing to monitor the efficiency of the infection. Upon *neuroLNC* overexpression TDP-43 localization remains largely nuclear, indicating that *neuroLNC* does not affect TDP-43 shuttling. Scale bars 20 µm. (**E**) Downregulation of TDP-43 assessed by qRT-PCR on C6 cells that were electroporated with either the control or the TDP-43 antisense construct (TDP-43-AS). TDP-43 expression is normalized to GAPDH and expressed as a percentage of the control. Statistical test: two-tailed Student t-test (** $P < 0.01$).

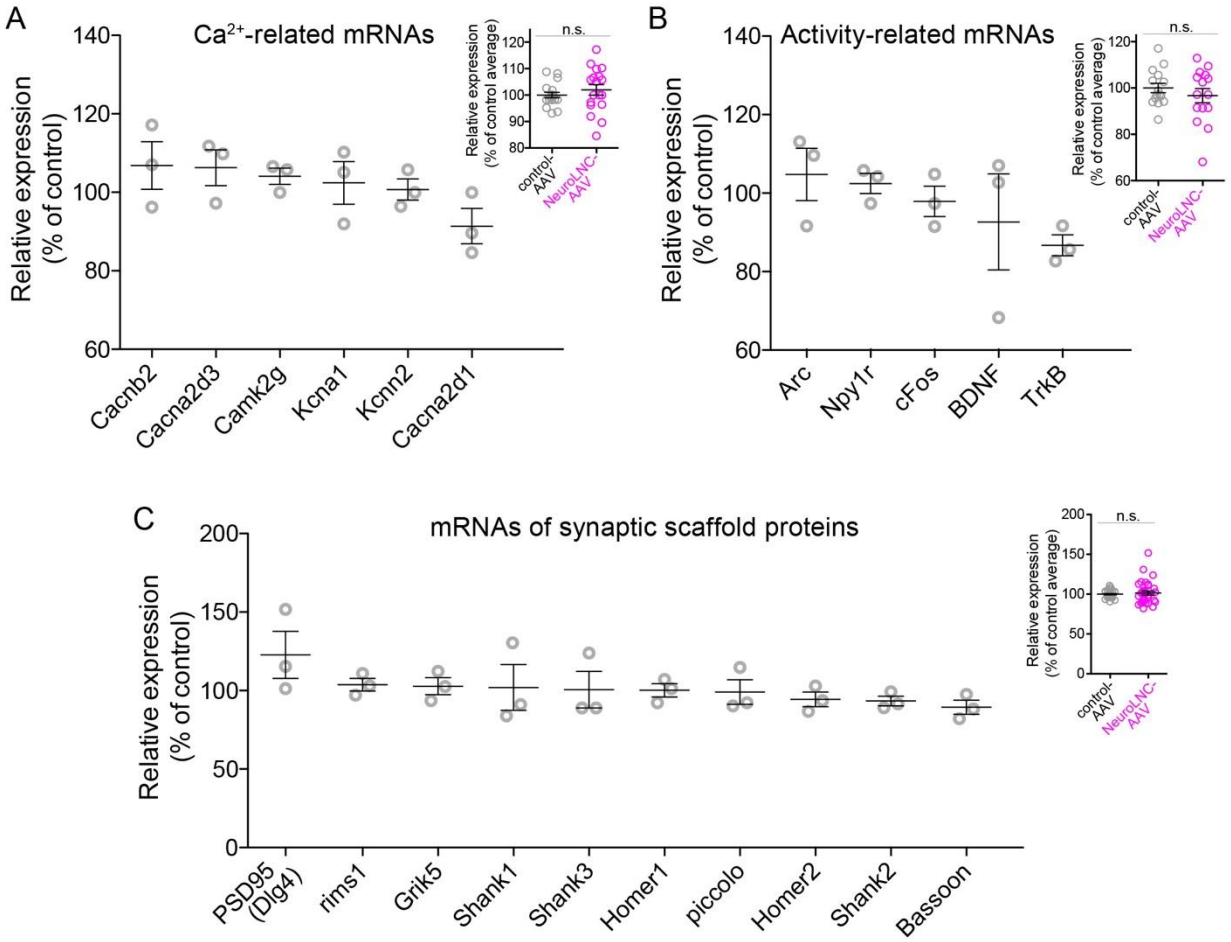

Fig. S6. *NeuroLNC* overexpression does not affect the expression of the mRNAs that encode for calcium-related pathways, neuronal activity, or synaptic scaffolds. (**A**-**C**) Results of the qRT-PCR following overexpression of *neuroLNC* in primary hippocampal neurons with an AAV. Data are GAPDH normalized and expressed as relative increase with respect to the control cultures (infected with a control AAV). Besides SV-associated mRNAs (**Fig. 6**), for all other classes of synaptic- or activity-related targets tested, no significant differences were observed neither at the level of single mRNAs nor at the level of the entire classes (insets on the right side of each graph).

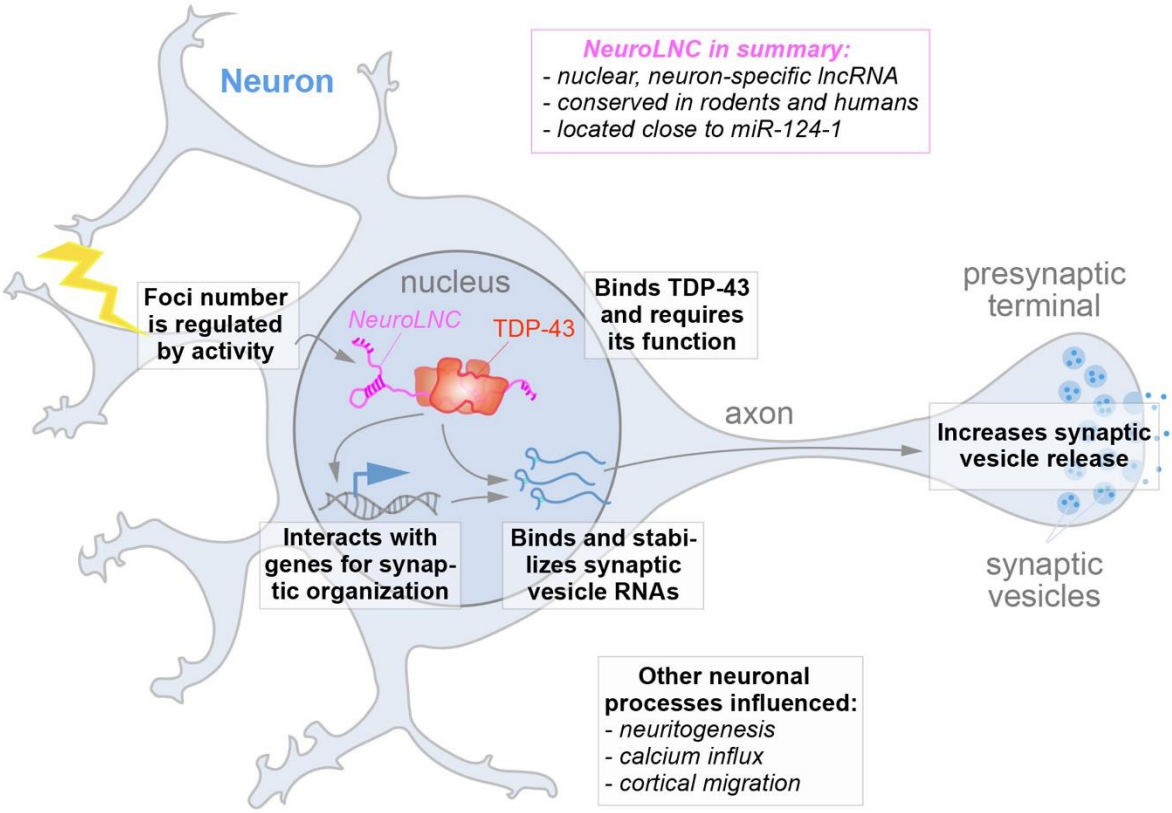

Fig. S7. Schematic representation summarizing the function of *NeuroLNC* in the nucleus of neurons.